# TAT Peptide Immobilization on Gold Surfaces: A Comparison Study with a Thiolated Peptide and Alkylthiols Using AFM, XPS, and FT-IRRAS

**Youngnam Cho[†] and Albena Ivanisevic*[,†,‡]**

*Department of Chemistry and Weldon School of Biomedical Engineering, Purdue University, West Lafayette, Indiana 47907*

*Received: September 20, 2004; In Final Form: December 8, 2004*

A TAT peptide was used to functionalize a gold surface by three different methods: adsorption from solution, microcontact printing, and dip-pen nanolithography (DPN). The composition and structure of the modified gold was characterized by atomic force microscopy (AFM), X-ray photoelectron spectroscopy (XPS), and Fourier transform −infrared reflection absorption spectroscopy (FT-IRRAS). We used two well-studied alkylthiols, mercaptohexadecanoic acid and 1-octadecanethiol, as a comparison in order to understand the structure of the TAT peptide monolayers prepared by the three methods. AFM studies allowed us to assess the homogeneity after each modification protocol. XPS was used to characterize the chemical composition of the gold surface after each functionalization procedure. The XPS results showed that surfaces modified with the TAT peptide by the three methods exhibit similar surface chemistry. Finally, FT-IRRAS experiments allowed us to conclude that the structure of the alkyl chains of the TAT peptides is fairly disordered and different after each procedure. Regardless of the type of surface functionalization method used, the monolayer of TAT peptide formed on the surface was of "liquidlike" nature.

## Introduction

The importance of fabricating nano- and micronscale features on surfaces has been recognized for the development of functional materials, sensors, and implantable devices.[1−3] In the past 25 years, the advancement of strategies to generate such structures has focused on the use of molecules that are useful in directing subsequent self-assembly events. In particular, a number of studies related to the structure of surface anchored molecules have been reported since the 1990s demonstrating the microscopic origins of the molecules' orientation. For example, monolayers composed of terminally functionalized alkanethiols, $X(CH_2)_nSH$ ($X = CH_3$, $CH_2OH$, $CH_2COOH$, $CH_2CO_2CH_3$, and $CH_2NH_2$), have been explored extensively, and detailed structural relationships have been deduced.[4−7] The advancements made in such studies have become the basis for the development of unconventional lithographic approaches such as microcontact printing and scanning probe lithography.[8,9] Furthermore, such approaches have inspired researchers to extend their capabilities to additional self-assembling monolayer (SAM) systems, such as thiolated biomolecules.[10−12] It has been established that the molecular orientation and ordering of the adsorbent in the SAMs is very important through studies utilizing biomolecules either in surface modification protocols or in lithographic methodologies. In particular, the way subsequent assembly processes take place is largely governed by the composition and structure of the modified surface.[13]

As the field of micro- and nanofabrication of SAMs is expanding, it is essential to develop protocols that allow one to compare and contrast the properties of structures generated with the same molecules by various methods. Critical parameters one needs to evaluate include size, shape, chemical composition, density, and conformation of the molecules after they have been immobilized on different surface types. Advancements in analytical instrumentation have made the assessments of some of these parameters fairly standard; however, the evaluation of the chemical composition and orientation of molecules in small pattern sizes (<1 micron) is not a trivial task. In a recent study, we described how to immobilize a TAT peptide on $SiO_x$ surfaces in the form of lithographic patterns.[14] TAT peptides are derived from the TAT protein of the human immunodeficiency virus type 1 (HIV-1). This protein has been linked through a variety of studies to important functions in cell permeation and viral replication.[15,16] Researchers have reported experiments demonstrating that short peptide sequences derived from this protein have recognition properties similar to the ones of the whole protein.[16] In our initial study, we described experiments that proved lithographic patterns composed of the TAT peptide retain their recognition properties with respect to a TAR RNA sequence.[14] However, in our experiments, we were not able to exclude the possibility that the TAR RNA is binding to the TAT peptide simply due to electrostatic interactions. To address this question, one needs to study the orientation of the molecules on the surface since their recognition properties are depended upon a particular conformation. Furthermore, such investigations can help determine the existence of differences in the orientation of the anchored molecules when various methods to immobilize them are used, e.g., adsorption from solution, microcontact printing, or scanning probe approaches. Such comparisons can be particularly useful in trying to decide how to functionalize complex architectures, such as microfabricated surfaces that can be used as novel analytical detection platforms, implantable devices, and/or biomedical sensors.[2]

The main focus of this study is to understand the TAT peptide adsorption process on gold surfaces. To our knowledge, no researchers have done an extensive study to compare the

* To whom correspondence should be addressed. E-mail: albena@purdue.edu.
[†] Department of Chemistry.
[‡] Weldon School of Biomedical Engineering.

10.1021/jp045731q CCC: $30.25 
Published on Web 03/15/2005

orientation of peptide molecules on gold by looking at surfaces modified by three different methods: adsorption from solution, microcontact printing, and dip-pen nanolithography (DPN).[17] To better understand the structure of the peptide on the chosen surface, we present a comparison between the TAT peptide and two well studied alkylthiols: 16-mercaptohexadecanoic acid (MHA) and 1-octadecanethiol (ODT). We characterize the composition and structure of the surfaces functionalized by the three methods using atomic force microscopy (AFM), X-ray photoelectron spectroscopy (XPS), and Fourier transform-infrared reflection absorption spectroscopy (FT-IRRAS). The experiments we describe allow us to verify the presence of the molecules on the surface and deduce the nature of molecular groups and their orientation.

## Experimental Section

**Reagents and Materials.** Gold(111) substrates were purchased from Molecular Imaging, Inc (Tempe, AZ). All gold substrates were fabricated from cleaved mica with epitaxially grown gold with a thickness of at least 1500 Å. 16-Mercaptohexadecanoic acid (MHA), 90%, and 1-octadecanethiol (ODT), 98%, were purchased from Aldrich. TRIS EDTA buffer at pH ~8.0 and phosphate-buffered saline (PBS) at pH ~6.5, were obtained from Sigma. The TAT peptide sequence (CGISYGRKKRRQRRR) was synthesized by Bio-Synthesis, Lewisville, TX where it was purified by HPLC and analyzed by MALDI-TOF.

**Surface Modification by Adsorption from Solution.** Individual gold substrates were cut into small pieces of $1 \times 1$ cm$^2$ and cleaned with a piranha solution (3:1 concentrated $H_2SO_4$: 30% $H_2O_2$, v:v) for a couple of seconds. *Caution: piranha solution reacts violently with organic solvents and should be handled with extreme care!* The surfaces were incubated for 24 h at 4−8 °C in a 100 $\mu$M solution of the TAT peptide prepared in PBS (pH ~ 6.5). Following this treatment, the surfaces were rinsed several times with the same buffer, washed multiple times with ultrapure water, and dried under nitrogen. MHA and ODT were dissolved in absolute ethanol to obtain a desired concentration, and the gold surfaces were immersed in a particular solution for 24−48 h. Subsequently, the surfaces were rinsed with ethanol and dried under nitrogen.

**Surface Modification by Microcontact Printing.** The three molecules used in this study, TAT peptide, MHA, and ODT, were immobilized on the gold surface using a PDMS stamp. The stamp was fabricated and inked using literature protocols.[8] The concentrations of the inking solutions are stated in the text. Ethanol was used as a solvent for MHA and ODT, and the TAT peptide was dissolved in PBS buffer (pH ~ 6.5). The stamp was brought in contact with the gold surface for ~5 s to generate the pattern. After the stamping, each surface was rinsed with solvent multiple times and dried with a stream of nitrogen.

**Surface Modification by DPN and AFM Characterization.** Multi-Mode Nanoscope IIIa from Digital Instruments, equipped with a Nanoscope software system, was used for all of the DPN patterning experiments and AFM imaging. The AFM probes used in the experiments, the "V" shaped triangular contact (model # MSCT-AUHW) and single beam shaped tapping mode tips (model # OMCL-AC16OTS-W2), were purchased from Veeco Instruments, CA. The contact mode tips and tapping mode tips had spring constants of 0.05 and 42 N/m, respectively. Contact mode AFM was used for the DPN patterning. All of the imaging experiments were performed under ambient conditions where the temperature and humidity ranged from 24 to 27 °C and 20% to 40%, respectively. Throughout the patterning experiments, the AFM instrument was placed in a home-built glovebox equipped with temperature and humidity controls. To pattern this particular ink, we had to increase the humidity to at least 75% in order to always obtain consistent and reproducible results. The ink solutions in this study were 2 mM ODT and 1 mM MHA solutions in ethanol and a 12 mM TAT peptide solution in PBS buffer (pH ~6.5). The patterning by MHA and ODT has been previously reported and reproduced for this study.[18] For the peptide solution, the tips were coated with peptide by briefly (5−60 s) placing them into an ink solution, rinsing them with buffer, and drying the backside of the cantilever using a clean filter paper. This procedure was repeated multiple times (3−4) prior to the DPN experiments and is described in more detail in our previous study.[14] The tips were immediately mounted onto the AFM tip holder and utilized in the lithography experiments. Prior to the DPN procedure, we calibrated each coated cantilever so that the applied force was 0 nN. During patterning, the scan parameters were fast scan lines of 512 with scan rates of 3.05 Hz (tip speed of either 30.5 $\mu$m/s when 5 $\mu$m scan sizes were used or 61.0 $\mu$m/s for 10 $\mu$m scan sizes). Either lateral force microscopy or tapping mode AFM (TMAFM) with clean tips at 90° scan direction was used to verify the DPN patterns prior to using the substrates for further experiments. Depending on the experimental conditions, the imaging was carried out with scan speeds of 2 to 4 Hz.

**Contact Angle Measurements.** Static contact angle measurements were performed using a Tantac, Inc Contact Angle Meter (model CAM-PLUS MICRO), and the angles were read by the half-angle method. For each measurement, a drop of water (1 $\mu$L) was delivered to the surface using a syringe equipped with a micrometer. The angle was measured within 30 s of the drop deposition. At least 5 measurements were done for a given surface and averaged.

**FT-IRRAS.** FT-IRRAS spectra from the gold substrates were collected in a single reflection mode with an FTIR spectrometer (Thermo Nicolet, Madison, WI). This instrument was coupled to a Continu$\mu$m IR microscope that allowed us to spectroscopically survey surfaces. The Continu$\mu$m had a motorized XYZ translation stage. The p-polarized light was incident at 80° from the surface normal to the substrate. A narrow-band mercury−cadmium−telluride (MCT) detector was used to detect the reflected light. The spectrometer and the microscope unit were interfaced with a computer, which uses Thermo Nicolet's OMNIC software that provides all of the tools necessary for the FT-IRRAS analysis. Spectra were collected from 1024 scans at a resolution of 4 cm$^{-1}$. The water in the sample compartment was purged with high purity nitrogen gas. An additional home-built chamber around the microscope unit was utilized to accomplish sufficient water exclusion. The data for the high- (2750 ~ 3100 cm$^{-1}$) and low-frequency regions (1500 ~ 1850 cm$^{-1}$) were acquired separately. All spectra of the monolayers formed by the TAT peptide and alkanethiols via the three methods were subtracted from the spectra for the bare Au substrate. For the FT-IRRAS experiments, DPN structures were generated next to one another to cover a total area of ~100 × 100 $\mu$m$^2$. A very large alignment marker was used to locate the patterned area. The Supporting Information section shows a detailed diagram of how the sample was prepared. All samples used in the FT-IRRAS measurements were subsequently characterized by XPS.

**XPS.** XPS survey and high-resolution scans were collected with a Kratos Axis ULTRA X-ray photoelectron spectrometer. The instrument was equipped with a monochromatic Al K$\alpha$ X-ray source, small area extraction optics, a spherical capacitor

**TABLE 1: Summary of the XPS Binding Energy Assignments for C 1s and N 1s for Three Different Ways the TAT Peptide Was Immobilized on the Surface**

| TAT peptide Immobilization on Au surfaces | C 1s BE (eV), %, assignment | N 1s BE (eV), % assignment |
|---|---|---|
| adsorption from solution | 283.7 (50.7), C-H | 398.5 (84.4), $NH_2$ |
| | 285.2 (27.2), C-N | 399.2 (15.6), amide-N |
| | 287.0 (21.1), amide-C | |
| microcontact printing | 283.0 (54.1), C-H | 398.0 (85.0), $NH_2$ |
| | 284.2 (32.1), C-N | 399.8 (15.0), amide-N |
| | 286.7 (13.8), amide-C | |
| DPN patterning | 283.1 (45.4), C-H | 398.0 (83.4), $NH_2$ |
| | 284.6 (35.5), C-N | 399.2 (16.6), amide-N |
| | 286.5 (19.1), amide-C | |

electron energy analyzer, and a dual channel plate position sensitive detector. Survey spectra were taken from 0 to 1100 eV with pass energy of 160 eV. High-resolution scans were collected with a pass energy of 40 eV. All XPS spectra are plotted based on the intensity obtained from the instrument and are shown as collected in order to represent signal-to-noise ratios. In figures where the data are presented as stacks, all of the plots have the same *y* scales. The data were always collected from the same location on the sample. In experiments where patterned surfaces were used, a micron-sized alignment marker was utilized in order to ensure that data was collected from specific patterned regions. For the XPS evaluation studies, DPN structures were generated next to one another to cover a total area of $\sim 100 \times 100\ \mu m^2$. The Supporting Information section shows a detailed diagram of how the sample was prepared. A stamp that generates structures with similar dimensions was used to fabricate surfaces for these studies. The survey and high-resolution scans on the modified substrates were collected from the same restricted region. Data treatment was done using a commercial software package, XPS PEAK (version 4.1). The peaks were fitted using a mixture of Gaussian and Lorenzian functions. The background was modeled using a Shirley function. The high-resolution spectra for C 1s and N 1s were fitted, and based on the peak area analysis, the data in Table 1 was compiled.

## Results and Discussion

**I. Surface Modifications.** Understanding how peptide molecules interact with various types of surfaces is of great importance for the development of new types of composite biomaterials and biosensors. To accelerate such developments, one needs to utilize various methodologies for surface modification. In some instances it is crucial to be able to consistently modify substrates through adsorption from solution, in other cases, it is important to be able to rapidly prototype micron scale patterns on a given surface, and in additional applications such as device modification, it is crucial to be able to place small patterns in complex architectures. To understand the advantages of each surface modification method, one needs to perform a systematic comparative study on a given surface with the molecules of interest. The recognition properties of the TAT peptide make it an ideal molecule for the integration in a variety of sensing platforms.[19] Our prior work with this molecule focused on patterning strategies on $SiO_x$ surfaces. However, to be able to compare the quality of various types of surface modifications, we decided to use gold as a substrate. Gold surfaces show high sensitivity with respect to FT-IRRAS as well as high affinity to bind to thiols. The properties of the gold surfaces have allowed researchers to investigate the immobilization of several thiol-containing molecules such as alkylthiols, thiol-modified ssDNA, thiol-containing proteins, and specifically engineered viruses.[4,10,11,20−23] The wealth of studies in the literature allow us to compare and contrast the surface modifications of the TAT peptide with two well studied alkylthiols: MHA and ODT.

The surface modification by adsorption from solution is easily done by allowing the surfaces to stay in a solution of the appropriate thiolated molecule for at least 24 h. We begin the experiments by immersing the gold substrates in solutions of 2 mM ODT, 1 mM MHA, and 4 mM TAT peptide for 24−48 h. The average contact angles were 30°, 110°, and 30°, for surfaces modified with 1 mM MHA, 2 mM ODT, and 4 mM peptide, respectively. In all cases, shorter exposure times resulted in irreproducible results. The wettability of the surface as a result of the adsorption of the two alkylthiols has been previously discussed in detail.[6] The long alkylthiols are expected to form oriented monolayers on the gold surface. The contact angles for the surfaces modified with MHA and ODT were in agreement with the literature.[4,6] In the case of the TAT peptide, the contact angle measurements suggest that upon attaching to the gold, presumably through the thiol group, the TAT peptide adapts a conformation that allows the carbonyl groups to stick away from the gold. Since the surfaces are fairly hydrophilic after the adsorption of the TAT peptide, it is reasonable to assume that the nitrogens from the amide bonds are closer to the gold surface and are capable of interacting with it. Due to this interaction, the peptide will be expected to rest flat on the gold surface. We used AFM, XPS, and FT-IRRAS to verify this hypothesis.

The quality of the monolayers we produce via adsorption from solution depends on the initial surface quality. Prior to the adsorption of the molecules, the gold surface was fairly smooth, rms $= 0.27 \pm 0.03$ nm. In the case of the TAT peptide, one would expect the peptide to attach to the gold surface through the thiol group on the cysteine residue. However, the flexibility of the molecule and its ability to adapt various conformations is likely to contribute to the formation of randomly oriented monolayers. Upon incubation in the ODT, MHA, and TAT peptide solutions, the rms values were $0.69 \pm 0.07$, $0.91 \pm 0.16$, and $0.84 \pm 0.30$ nm, respectively. These results are consistent with what one would anticipate to observe based on the structures of the molecules: ODT is expected to form the most ordered monolayer due to its straight alkyl chains; MHA is likely to produce less ordered monolayers compared to ODT due to the steric hindrance provided by its carboxylic acid group; and the TAT molecules can adapt various conformations and are likely to produce disordered monolayers. Disordered monolayers are more likely to lead to clustering of the peptides on the surface. If clustering of the peptides is taking place, one can expect that the surfaces will become hydrophilic. A contact angle of 30° supports the possibility of this taking place, eventually leading to subsequent formation of multilayers of TAT peptides on the gold.

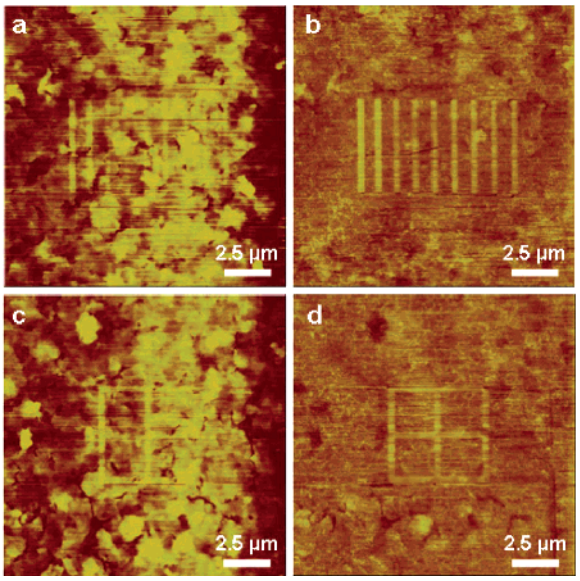


**Figure 1.** (a and c) Height and (b and d) LFM images of a Au surface containing DPN patterns terminated with a TAT peptide. The ink solution used to coat the tip had a concentration of 12 mM. All images were collected with a scan size of 15 × 15 $\mu m^2$ and scan rate of 3.05 Hz. The LFM data scale is 60 mV and height scale is 5 nm.

The gold surfaces were also modified using a PDMS stamp inked with each molecule. The stamp we used was large enough ($\sim 0.5 \times 0.5$ $cm^2$) so that the area modified with the molecules of interest can be used to perform contact angle measurements. The stamp was flat and had no patterns since the main goal of this study was to compare the way the molecules orient on the surface as a result of the three different modification procedures. The contact angles after the surfaces were modified by microcontanting printing were the same as after the surfaces were modified by adsorption from solution. The patterned area of the surface was also evaluated by AFM. The average rms values extracted from 3 to 4 randomly chosen 1 × 1 $\mu m^2$ images on the patterned areas were 0.99 ± 0.39, 1.12 ± 0.68, and 0.80 ± 0.15 nm for surfaces stamped with ODT, MHA, and the TAT peptide, respectively. The results so far indicate that the TAT peptide produces the same quality of modified gold substrates regardless of whether one modifies the surface via adsorption from solution or stamps the peptide on the surface using an elastomer stamp.

The procedure for DPN patterning of ODT and MHA on gold is well documented in the literature by several different research groups.[24−28] We have reproduced the patterning of MHA and ODT (see the Supporting Information) for the XPS and FT-IRRAS comparative studies (see below). Our earlier study demonstrated the successful DPN writing of the TAT peptide ink on functionalized $SiO_x$ surfaces.[14] The scheme for the patterning of the TAT peptide on the Au surface is straightforward since one does not need to modify the gold surface and can use the thiol on the cysteine residue for attachment. The DPN patterning of the TAT peptide on gold was performed under the same experimental conditions as in our earlier work.[14] Figure 1 displays typical patterning results on the gold substrate. Immediately after the writing, the patterns were imaged to collect height and lateral force microscopy (LFM) images with a clean tip.

The average width of the lines was around 500 nm, whereas the average height was approximately 1 nm. The written TAT peptide structures appeared lighter than the bare gold in all LFM images. Thus, the LFM images collected with a clean tip suggest that the TAT peptide patterns are hydrophilic. Based on the data shown in Figure 1 and what has been reported in the literature regarding the DPN patterning of ODT and MHA, there are some important differences between the DPN patterns composed of the alkylthiols and the peptide. One can clearly see the TAT peptide features in the height images and measure the height of the structures to be approximately 1 nm. In addition, despite the fact that the clean gold surface was fairly hydrophilic (contact angle of ~20°), we needed to increase the humidity to at least 75% in order to be able to deliver the peptide molecules to the surface. Previously, we reported a procedure for the writing of TAT peptides on the hydrophobic surfaces.[14] In our previous studies and in the present report, we observed that the high humidity is a critical component for the successful delivery of these molecules to the surface. The mechanism of molecular ink transport during the DPN process has been modeled by Jang et al. and is thought to include molecular deposition, diffusion, and surface binding events.[29] Our observations so far strengthen the hypothesis that the DPN delivery of the TAT peptide molecular ink to any type of surface (hydrophilic or hydrophobic) is through a mechanism that is dominated by molecular deposition rather than lateral diffusion or surface binding events that might apply to alkythiol molecules. The transport properties of the TAT peptide ink are not the subject of this paper but are very important for a variety of applications and will be described in future studies.

**II. Surface Characterization.** After the initial characterization performed by AFM and contact angle measurements, we used XPS and FT-IRRAS to assess the quality of the surfaces after each type of modification. The techniques we used allowed us to deduce the chemical composition of the surfaces and begin to understand the arrangement of molecules on the surface. A similar characterization protocol has been used by Boland et al. to compare microcontact printing and ink-jet printing of biomolecules.[30]

*XPS Characterization.* We opted to use XPS to characterize our surfaces for several reasons. Initially, this technique was utilized to verify the presence of each molecule on the gold upon modification by the three different methodologies. Furthermore, this technique allowed us to compare the relative amounts of each element on a surface of interest. Finally, XPS allows for the extraction of some structural information with respect to the molecules on the surface since binding energies' shifts can be used to compare oxidation states. At the beginning of each surface characterization experiment, we collected core-level survey spectra of the modified surfaces by each method. In all cases, a clean gold surface was used as a reference. These survey spectra, an example of which is shown in Figure 2, confirm the presence of Au 4d, Au 4f, Au 4p, C 1s, N 1s, and O 1s on all modified surfaces. Additional survey spectra are available in the Supporting Information and show results similar to previously reported studies on gold. It is important to note that even in the survey spectrum of the surface modified via DPN with the TAT peptide one can distinguish the presence of nitrogen. To understand the structure of species present on the surface, high-resolution spectra were recorded for the main core-level peaks of gold, sulfur, carbon, oxygen and nitrogen.

The sulfur signal is of interest because thiolated molecules are normally anchored through the sulfur onto the gold. The high resolution spectra of S 2p can reveal whether the thiol headgroups of the molecules form a covalent bond through the sulfur or not. It is well-known that the binding energy range generating covalent bonds between the sulfur and the gold surface is typically beeetween 161.5−162.5 eV.[5,6,12,31−33] Compared to this reference value, it is notable that MHA and ODT

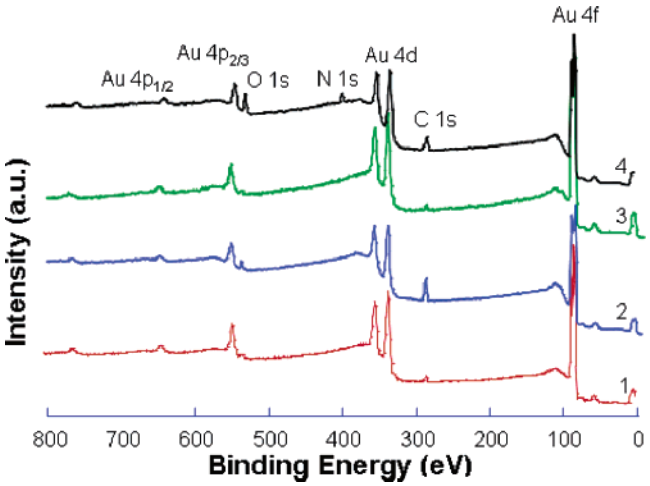


**Figure 2.** XPS survey spectra of (1) clean Au; (2) Au patterned with MHA by DPN; (3) Au patterned with ODT by DPN; and (4) Au patterned with TAT peptide by DPN.

on surfaces modified by adsorption from solution bind covalently through the Au−S bond. In addition, ODT was also observed to anchor on the surface through the Au−S bond when microcontact printing and DPN were utilized to modify the surface. However, in the case of MHA when surfaces were functionalized via microcontact printing and DPN, peaks located at 163.5 and 170 eV were observed, indicating the presence of unbound sulfur on the gold surface as well as −S−O− species. Most likely, the −S−O− species are formed as a result of the oxidation of the molecules after they are delivered to the surface. In the case of the TAT peptide, the high-resolution spectra of S 2p after the modification procedures showed a peak at 171.3 eV. This result indicates that the sulfur species on the peptide are more susceptible to oxidation. Previously, we observed that in order for the TAT peptides to remain permanently on the surface, we needed to let the lithographically modified surfaces "age" for at least 24 h. This "aging" process allows the coupling chemistry to take place. During this time, some of the species on the surface can oxidize. Based on our XPS analysis, it appears that the S binds to the gold surface and the oxidation process does not seem to stabilize the attachment of the peptide to the gold. All surfaces we examined were irreversibly modified with the TAT peptide since repeated washings with water did not remove the peptide from the surface.

The line shapes of the high-resolution C 1s core level spectra for MHA and ODT showed no differences when data from the three surface modification methods were compared. In the case of ODT a single peak centered at 283.5 eV was observed which is consistent with the presence of hydrocarbon chains on the surface. For surfaces functionalized with MHA, a sharp peak at 285.7 eV was recorded, and an additional peak at 290.3 eV confirmed the existence of functionalized C atoms on the surface.[34] In the case of the TAT peptide, the high-resolution C 1s and N 1s core level spectra can provide the most information with respect to the composition and structure of the modified gold. The high-resolution data for all three methodologies used to functionalize the gold with the TAT peptide are summarized in Figure 3. The peaks for both elements are broad and therefore can be deconvoluted. A summary of the deconvolution results is presented in Table 1. The C 1s spectra on each type of surface showed the following functionalities: C−H, C−N, and amide-C. In particular, the presence of amides on the surfaces causes the appearance of a shoulder in the C 1s spectra at a higher binding energy. The presence of this shoulder has been well documented in the literature to be

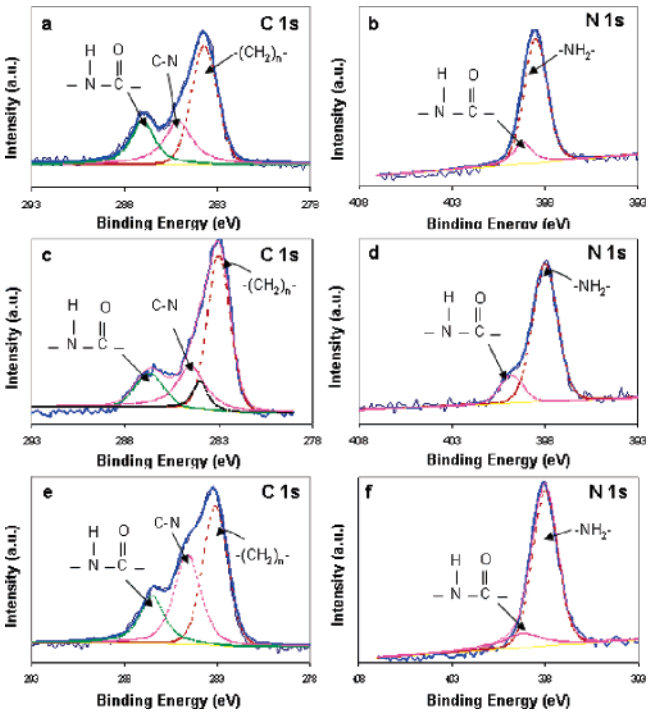


**Figure 3.** (a and b) High-resolution XPS for C 1s and N 1s spectra surface deconvolution analysis of a Au surface modified with the TAT peptide by adsorption from solution. (c and d) High-resolution XPS for C 1s and N 1s spectra surface deconvolution analysis of a Au surface modified with the TAT peptide by microcontact printing. (e and f) High-resolution XPS for C 1s and N 1s spectra surface deconvolution analysis of a Au surface modified with the TAT peptide by DPN.

caused by electronegative substituents on the carbon.[4,34] The data in Table 1 shows that the relative percentages of the various species comprising the C 1s spectra are different on surfaces modified with the TAT peptide by each functionalization methodology. These differences can be attributed to the variable amount of molecules after each modification method. The orientation of the peptides once they are anchored on the surface can also contribute to these differences. FT-IRRAS measurements can be used to verify this hypothesis (see below).

The high-resolution N 1s core level spectra indicate the presence of $NH_2$ and amide-N on surfaces modified with the TAT peptide by all three methods, Figure 3. The relative percentages of each species are similar, Table 1. One notable difference on surfaces functionalized by microcontact printing with the peptide is the appearance of a shoulder peak at 399.8 eV. In Table 1, this binding energy is attributed to the presence of amide-N. However, part of this shoulder peak can also be due to the presence of protonated amine groups ($NH_3^+$). The $NH_3^+$ species have been shown to exhibit binding energies in the range of 399.8−401.7 eV.[10] Taken in its entirety the XPS data demonstrate that the gold surfaces modified with the TAT peptide by the three methodologies have similar composition based on the elements present on the surface. High-resolution analysis of the core level spectra of S 2p, C 1s, and N 1s suggest that the organization of the molecules on the surface is different depending on each type of modification used to anchor the TAT peptides on the gold.

*FT-IRRAS Characterization.* Of the variety of surface characterization techniques available, FT-IRRAS is particularly useful and powerful due to its ability to provide information with regard to orientation and composition of molecules anchored on metal surfaces.[35] In this study, FT-IRRAS allowed us to determine the chemical nature of the adsorbed species

and their molecular arrangement when three different methodologies were used to modify the same surface with the same molecules. The most important question we were trying to address was whether the surface bound films composed of the TAT peptide molecules are "liquidlike" or "crystalline-like" in nature. This technique allowed us to observe that the nature of the surface-anchored TAT peptide layers changes when each surface functionalization method is used.

Prior to discussing the FT-IRRAS results we obtained, we note some important features of each molecule obtained from solution FT-IR experiments in transmission mode. Solution IR experiments with these molecules have been discussed in the literature[4,34,36] and are shown in the Supporting Information. The peak positions of $\upsilon(CH_2)$ can provide direct evidence to distinguish between "liquidlike" or "crystalline-like" packing of the alkyl chains.[4,5,7,30,37,38] The high-frequency region of the IR spectrum can explain the structural organization of the alkyl chains. The two $CH_2$ C−H stretching modes, $\upsilon_{as}$ ($CH_2$) and $\upsilon_s$ ($CH_2$), are observed at 2925 and 2853 $cm^{-1}$, 2923 and 2852 $cm^{-1}$, and 2922 and 2851 $cm^{-1}$ in the solution FT-IR spectra for MHA, ODT, and the TAT peptide, respectively. Another important feature in this region is the $CH_3$ C−H stretching mode positioned at 2954 and 2955 $cm^{-1}$ in the solution IR spectrum of ODT and the TAT peptide, respectively. The small number of the terminal methyl groups causes the intensity of this peak to be low. Previous studies have shown that the frequency of the $\upsilon_{as}(CH_2)$ band in crystalline-like bulk is positioned at 2920 $cm^{-1}$ whereas the $\upsilon_s(CH_2)$ band is positioned at 2850 $cm^{-1}$.[4,7] However, in the liquidlike state, the position of $\upsilon_{as}(CH_2)$ is 2∼5 $cm^{-1}$ higher than in the crystalline-like state, whereas in the liquidlike state, the $\upsilon_s(CH_2)$ is 2∼3 $cm^{-1}$ higher than in the crystalline-like state. The low-frequency region (1500∼1850 $cm^{-1}$) can provide more details with respect to the structure of the TAT molecules. Strong and broad bands corresponding to the C═O stretching mode can be observed at 1819 and 1754 $cm^{-1}$. In addition, the peptide solution IR spectrum reveals strong amide I and II modes appearing at 1662 and 1540 $cm^{-1}$, respectively.

Initially we compared the FT-IRRAS spectra of gold surfaces modified by MHA and ODT by the three different methods, Figure 4. Spectra collected on surfaces modified by each method showed differences when compared to the solution FT-IR data. The peak positions for surfaces modified by adsorption from solution shifted toward higher frequencies in the case of the $\upsilon_{as}(CH_2)$ and toward lower frequencies in the case of $\upsilon_s(CH_2)$. This observation suggests that the alkyl chains in our monolayer films are loosely packed and exhibit liquidlike properties. A number of authors have reported crystalline lattices using these compounds.[39] However, experiments we performed and prior reports in the literature[4] indicate that disordered monolayers are more likely to form when the quality and uniformity of the gold surface decreases. In addition, researchers have described that the structure and orientation of the monolayers is dependent upon a number of conditions such as concentration, solvent identity, soaking time, temperature, and the initial quality of the surface used.[39] The data shown in Figure 4 represents the spectra collected on gold pieces cut from the same large commercially available substrate and used in the three different surface functionalization experiments. Surfaces modified with MHA and ODT by microcontact printing and DPN exhibited much smaller peak position changes toward lower frequencies and showed a narrower peak width. In the case of MHA, surfaces modified by microcontact printing showed the following $-CH_2$ bands: $\upsilon_{as}(CH_2)$ at 2918 $cm^{-1}$ and $\upsilon_s(CH_2)$ at 2850 $cm^{-1}$,

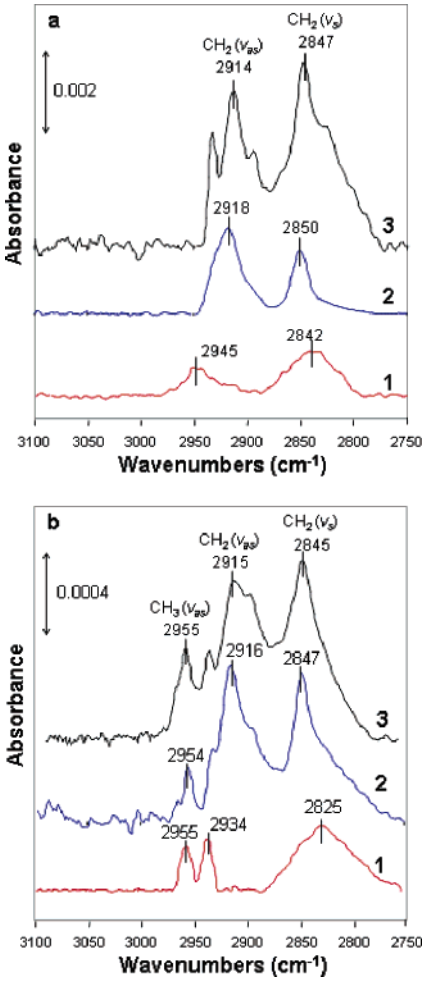


**Figure 4.** FT-IRRAS spectra of (a) gold surfaces functionalized with MHA by (1) adsorption from solution; (2) microcontact printing; and (3) DPN; (b) gold surfaces functionalized with ODT by (1) adsorption from solution; (2) microcontact printing; and (3) DPN.

whereas surfaces modified by DPN showed the following $-CH_2$ bands: $\upsilon_{as}(CH_2)$ at 2914 $cm^{-1}$ and $\upsilon_s(CH_2)$ at 2847 $cm^{-1}$. In the case of ODT, surfaces modified by microcontact printing showed the following $-CH_2$ bands: $\upsilon_{as}(CH_2)$ at 2916 $cm^{-1}$ and $\upsilon_s(CH_2)$ at 2847 $cm^{-1}$, whereas surfaces modified by DPN showed the following $CH_2$ bands: $\upsilon_{as}(CH_2)$ at 2915 $cm^{-1}$ and $\upsilon_s(CH_2)$ at 2845 $cm^{-1}$. These observations indicate the formation of a "crystalline-like" packing of the alkyl chains on the gold after microcontact printing and DPN. Previous studies have shown that alkanethiols in crystalline-natured SAMs adapt all-trans conformational order due to the effect of the high-packing density.[4,34,36] Broad peak widths and shifts to higher frequency indicate the formation of a less dense and more disordered SAM. There are two structural groups that must be considered in all of the cases shown in Figure 4: $-CH_2-$ and $-CH_3$. Both of these structural groups contribute to the C−H stretching modes and can be either symmetric or asymmetric. In cases where the monolayer is rather disordered, shifts in these stretching frequencies and broadening of the bands can make it difficult to assign the origin of each peak in the spectra. Therefore, we contribute the shift in what appears to be the asymmetric peak to be due to the highly disorganized chains in the monolayer. Taken in sum, the data in Figure 4 supports the notion that one produces significantly different intermolecular environments when each one of the surface functionalization methods is used.

In subsequent experiments we collected FT-IRRAS on surfaces modified with the TAT peptide by each modification

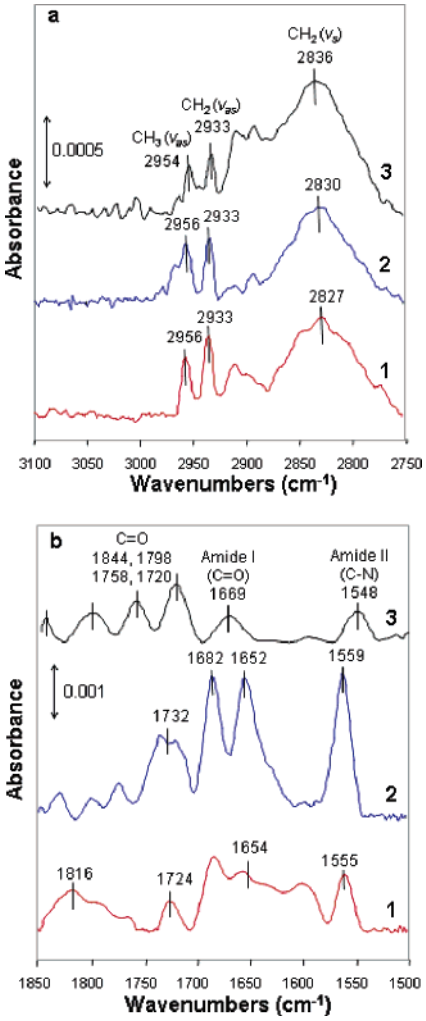


**Figure 5.** FT-IRRAS spectra of (a) the high-frequency region and (b) the low-frequency region of gold surfaces functionalized with the TAT peptide by (1) adsorption from solution; (2) microcontact printing; and (3) DPN.

method, Figure 5. The high-frequency regions of the spectra show the presence of hydrocarbon chains based on a broad peak centered at 2827, 2830, and 2836 $cm^{-1}$, after the TAT peptide was adsorbed from solution, microcontant printed, and delivered by DPN on the gold, respectively. The C−H peak positions are different when compared to the solution FT-IR spectrum of the TAT peptide. In addition, the ratio of the intensities of $\upsilon(CH_3)$:$\upsilon(CH_2)$ is significantly different. The asymmetric stretch has been used to distinguish if a sample is crystalline or liquidlike in nature.[36] The data we collected, Figure 5a, shows the $\upsilon_{as}(CH_2)$ at 2933 $cm^{-1}$ after the surface was functionalized by all three methods. Direct comparison of this region of the FT-IRRAS spectra with the solution FT-IR allows us to conclude that the structure of the alkyl chains is fairly disordered and the monolayer of TAT peptide formed on the surface is of "liquidlike" nature regardless of what type of surface functionalization method is used.

The analysis of the low-frequency region reveal further details regarding the organization of the peptide molecules on the surface, despite the fact that the band intensity is weak. The analysis of this low-frequency region provides information about the trans conformation of the amide and the interchain hydrogen bonding.[40,41] Based on these literature reports, hydrogen bonding occurs around ∼1550−1560 $cm^{-1}$ for an amide with a polymethylene structure, while non-hydrogen bonding appears around ∼1510 $cm^{-1}$. The data shown in Figure 5b indicates that interchain hydrogen bonding among amide groups is present. One can observe only one type of hydrogen bonded amide after each modification procedure in the region where the hydrogen bonding is expected to appear. These results are indicative of surface anchored molecules with liquid-like chains stabilized by hydrogen bonding. One of the most significant regions is between 1600 and 1700 $cm^{-1}$ due to the expected presence of the amide I band corresponding to the carbonyl stretching.[21] The amide I bands recorded after (i) adsorption from solution, (ii) microcontact printing, and (iii) DPN patterning appear at (i) 1654 and 1682 $cm^{-1}$, (ii) 1652 and 1682 $cm^{-1}$, and (iii) 1669 $cm^{-1}$, respectively. All of these bands are very broad and indicate a high degree of disorder. The amide II band, arising from the N−H stretching, is expected between 1500 and 1600 $cm^{-1}$.[42] The amide II bands recorded after (i) adsorption from solution, (ii) microcontact printing, and (iii) DPN patterning appear at (i) 1555 $cm^{-1}$, (ii) 1559 $cm^{-1}$, and (iii) 1548 $cm^{-1}$, respectively. On all surfaces, these bands represent the interchain hydrogen bonding. The data in Figure 5b contrasts each modification procedure and shows considerable differences in the amide I and II band positions. These differences indicate the variable intermolecular environments the TAT peptide participates in, after the surfaces are functionalized by each methodology. In addition to the amide stretching bands, obvious bands between 1700 and 1850 $cm^{-1}$ are observed. These bands correspond to the carbonyl stretching vibration bands. The C═O due to the structure of the side chains of the TAT peptide appear as very broad peaks in the region between 1720 and 1845 $cm^{-1}$. The position of these bands varies on the surfaces functionalized by each method. This observation is expected since there is a mutual relationship between the bond stretching frequencies and changes taking place in the intermolecular environment.[4] The differences in the peak positions and width after each preparation method imply that the TAT peptide molecule is structurally flexible on the surface, despite the fact that the XPS data show similar surface chemical composition after each modification.

## Conclusion

The data we present allows us to report the following: (i) A protocol that results in a gold surface modified with TAT peptide molecules. The gold surface can be functionalized with the TAT peptide by adsorption from solution, microcontact printing and DPN. Two well studied alkanethiols, MHA and ODT, were used to compare the quality of the surfaces modified with the peptide. (ii) The presence of all molecules on the gold surface was verified by XPS. The XPS results showed that surfaces modified with the TAT peptide by the three methods exhibit similar surface chemistry and homogeneity. (iii) FT-IRRAS spectroscopic characterization of the surfaces functionalized by each method allowed us to evaluate the way "rigid" alkanethiols form surface structures vs the flexible thiolated biomolecule, the TAT peptide. The FT-IRRAS data indicated that regardless of the surface modification method chosen the TAT peptides exhibit "liquidlike" or disordered packing. These results suggest that the molecules of TAT peptide in the SAMs have increased tilt angle from the surface normal.

**Acknowledgment.** This work was supported by the Bindley Biosciences Center at Purdue University and by NASA under award No. NCC 2-1363. Any opinions, findings, and conclusions expressed in this material are those of the authors and do not necessarily reflect the views of the National Aeronautics and Space Administration. The authors acknowledge experi-

mental help from Dr. Richard Haasch (UIUC) to carry out the XPS characterization. All XPS experiments were performed at the Center for Microanalysis of Materials, UIUC, which is partially supported by U. S. Department of Energy under grant DEFG02-96-ER45439.

**Supporting Information Available:** AFM images of patterns generated via DPN using MHA and ODT as inks; XPS survey spectra after the surfaces were modified by adsorption from solution or by microcontact printing with each of the three molecules; FT-IR solution data for the high-frequency and low-frequency region for each of the three molecules; high-resolution images of the bare Au (111) surface; and a schematic representation of the fabrication of surfaces used for the characterization studies. This material is available free of charge via the Internet at http://pubs.acs.org.

## References and Notes

(1) Aizenberg, J. *Adv. Mater.* **2004**, *16*, 1295−1302.
(2) Raghavan, S.; Chen, C. S. *Adv. Mater.* **2004**, *16*, 1303−1313.
(3) Jeon, S.; Menard, E.; Park, J. U.; Maria, J.; Meitl, M.; Zaumseil, J.; Rogers, J. A. *Adv. Mater.* **2004**, *16*, 1369−1373.
(4) Nuzzo, R. G.; Dubois, L. H.; Allara, D. L. *J. Am. Chem. Soc.* **1990**, *112*, 558−569.
(5) Li, Z.; Chang, S. C.; Williams, R. S. *Langmuir* **2003**, *19*, 6744−6749.
(6) Laibinis, P. E.; Whitesides, G. M.; Allara, D. L.; Tao, Y. T.; Parikh, A. N.; Nuzzo, R. G. *J. Am. Chem. Soc.* **1991**, *113*, 7152−7167.
(7) Nakano, K.; Sato, T.; Tazaki, M.; Takagi, M. *Langmuir* **2000**, *16*, 2225−2229.
(8) Xia, Y.; Rogers, J. A.; Paul, K. E.; Whitesides, G. M. *Chem. Rev.* **1999**, *99*, 1823−1848.
(9) Kramer, S.; Fuierer, R. R.; Gorman, C. B. *Chem. Rev.* **2003**, *103*, 4367−4418.
(10) Xiao, S.-J.; Textor, M.; Spencer, N. D. *Langmuir* **1998**, *14*, 5507−5516.
(11) Petrovykh, D. Y.; Kimura-Suda, H.; Tarlov, M. J.; Whitman, L. J. *Langmuir* **2004**, *20*, 429−440.
(12) Petrovykh, D. Y.; Kimura-Suda, H.; Whitman, L. J.; Tarlov, M. J. *J. Am. Chem. Soc.* **2003**, *125*, 5219−5226.
(13) Geissler, M.; Xia, Y. *Adv. Mater.* **2004**, *16*, 1249−1269.
(14) Cho, Y.; Ivanisevic, A. *J. Phy. Chem. B* **2004**, *108*, 15223−15228.
(15) Fawell, S.; Seery, J.; Daikh, Y.; Moore, C.; Chen, L. L.; Pepinsky, B.; Barsoum, J. *Proc. Natl. Acad. Sci. U.S.A.* **1994**, *91*, 664−668.
(16) Long, K. S.; Crothers, D. M. *Biochemistry* **1995**, *34*, 8885−8895.
(17) Ginger, D. S.; Zhang, H.; Mirkin, C. A. *Angew. Chem., Int. Ed.* **2004**, *43*, 30−45.
(18) Hong, S.; Zhu, J.; Mirkin, C. A. *Langmuir* **1999**, *15*, 7897−7900.
(19) Tassew, N.; Thompson, M. *Anal. Chem.* **2002**, *74*, 5313−5320.
(20) Kimura-Suda, H.; Petrovykh, D. Y.; Tarlov, M. J.; Whitman, L. J. *J. Am. Chem. Soc.* **2003**, *125*, 9014−9015.
(21) Pradier, C.-M.; Salmain, M.; Liu, Z.; Methivier, C. *Surf. Interface Anal.* **2002**, *34*, 67−71.
(22) Stapleton, J. J.; Harder, P.; Daniel, T. A.; Reinard, M. D.; Yao, Y.; Price, D. W.; Tour, J. M.; Allara, D. L. *Langmuir* **2003**, *19*, 8245−8255.
(23) Hu, J.; Liu, Y.; Khemtong, C.; Khoury, J. M. E.; McAfoos, T. J.; Taschner, I. S. *Langmuir* **2004**, *20*, 4933−4938.
(24) Piner, R. D.; Zhu, J.; Xu, F.; Hong, S.; Mirkin, C. A. *Science* **1999**, *283*, 661−663.
(25) Hyun, J.; Ahn, S. J.; Lee, W. K.; Chilkoti, A.; Zauscher, S. *Nano Lett.* **2002**, *2*, 1203−1207.
(26) Weeks, B. L.; Noy, A.; Miller, A. E.; DeYoreo, J. J. *Phys. Rev. Lett.* **2002**, *88*, 255505−255501−255505−255504.
(27) Sheehan, P. E.; Whitman, L. J. *Phys. Rev. Lett.* **2002**, *88*, 156104−156101−156104−156104.
(28) Barsotti, R. J.; O'Connell, M. S.; Stellacci, F. *Langmuir* **2004**, *20*, 4795−4798.
(29) Jang, J. Y.; Hong, S.; Schatz, G. C.; Ratner, M. A. *J. Chem. Phys.* **2001**, *115*, 2721−2729.
(30) Pardo, L.; Wilson, W. C.; Boland, T. *Langmuir* **2003**, *19*, 1462−1466.
(31) Winter, R.; Nixon, P. G.; Gard, G. L.; Graham, D. J.; Castner, D. G.; Holcomb, N. R.; Grainger, D. W. *Langmuir* **2004**, *20*, 5776−5781.
(32) Yam, C.-M.; Pradier, C.-M.; Salmain, M.; Marcus, P.; Jaouen, G. *J. Colloid Interface Sci.* **2001**, *235*, 183−189.
(33) Love, J. C.; Wolfe, D. B.; Haasch, R.; Chabinyc, M. L.; Paul, K. E.; Whitesides, G. M.; Nuzzo, R. G. *J. Am. Chem. Soc.* **2003**, *125*, 2597−2609.
(34) Bain, C. D.; Troughton, E. B.; Tao, Y. T.; Evall, J.; Whitesides, G. M.; Nuzzo, R. G. *J. Am. Chem. Soc.* **1989**, *111*, 321−335.
(35) Golden, W. G.; Saperstein, D. D.; Severson, M. W.; Overend, J. *J. Phys. Chem.* **1984**, *88*, 574−580.
(36) Porter, M. D.; Bright, T. B.; Allara, D. L.; Chidsey, C. E. D. *J. Am. Chem. Soc.* **1987**, *109*, 3559−3568.
(37) Azzam, W.; Wehner, B. I.; Fischer, R. A.; Terfort, A.; Woll, C. *Langmuir* **2002**, *18*, 7766−7769.
(38) Jennings, G. K.; Yong, T.-H.; Munro, j. C.; Laibinis, P. E. *J. Am. Chem. Soc.* **2003**, *125*, 2950−2957.
(39) Ulman, A. *Chem. Rev.* **1996**, *96*, 1533−1554.
(40) Tam-Chang, S. W.; Biebuyck, H. A.; Whitesides, G. M.; Jeon, N.; Nuzzo, R. G. *Langmuir* **1995**, *11*, 4371−4382.
(41) Clegg, R. S.; Hutchison, J. E. *Langmuir* **1996**, *12*, 5239−5243.
(42) Uvdal, K.; Vikinge, T. P. *Langmuir* **2001**, *17*, 2008−2012.